Bulletin of Electrochemistry 1 (6) Nov.-Dec. 1985, pp. 603-608

# LINEAR SWEEP VOLTAMMETRIC SIMULATION OF MONOLAYER FORMATION - I ADSORPTION, NUCLEATION - GROWTH - OVERLAP AND COMBINED MODELS WITH UNIFORM SURFACE SITES

*M NOEL, C A BASHA AND S CHANDRASEKARAN*
Central Electrochemical Research Institute, Karaikudi - 623 006

**ABSTRACT**

A generalised overview of the linear sweep voltammetric (LSV) simulation of adsorption model (AM) and nucleation - growth - overlap model (NGOM) is presented, along with the numerical simulation of LSV response for the combined model. The numerical simulation indicates that separate voltammetric peaks may not be obtained if the surface sites are uniform and no heterogeneity effects are introduced by the surface coverage. However, some specific features of th surface coverage may be used to distinguish this model from AM to NGOM. These aspects are discussed in detail.

**Key words: Linear sweep voltammetry, adsorption, nucleation.**

## 1. INTRODUCTION

Although the nature of the electrode material can influence the kinetics of many electrochemical processes, monolayer formation processes offer a unique opportunity to study the influence of electrode surface in detail. A metal ion such as $Pb^{2+}$ on reduction at a noble metal such as Pt can form a monolayer film of Pb atoms on Pt surface. This deposition process takes place at potentials much more positive than the bulk deposition potentials. This positive shift due to the thermodynamic stability may be as high as 400 mV or more. Many other metal ions such as bismuth, thallium, cadmium and zinc may form such monolayers on more noble metal substrates such as Cu, Ag, Au or Pb [1 - 4]. Hydrogen also can form a monolayer on substrate metals such as Pt and Rh [5 - 8]. $OH^-$ oxidation on practically all noble metals can form M − OH as well as MO layers at distinct potential regions much more negative than bulk oxidation or oxygen evolution region [5 - 8].

Studies on such monolayers can result in useful correlation between the nature of electrode material (say work function) and their electrochemical behaviour (say difference between monolayer and bulk deposition potential) [1]. These monolayers can also play a very important role in improving the electrocatalytic behaviour of the substrate metals.

Linear sweep voltammetry (LSV) and cyclic voltammetry (CV) have been extensively used to characterise this monolayer formation and dissolution. The monolayer formation may proceed at random on the substrate lattice. This mode of monolayer formation is termed as adsorption model (AM) and most of the H and O monolayer [5 - 8] and some metal monolayer formation [1 - 2] studies presume this model. However, there are some clear-cut evidences from chronoamperometry that the monolayer formation proceeds via formation of (two dimensional) nuclei of a certain size followed by lateral growth up to overlap of these centres [3 - 4]. This model is called the nucleation-growth and overlap model (NGOM). Theoretical derivations numerical simulations for LSV technique have been derived from both AM [9 - 11] and NGOM [12 - 15] and reviewed recently [16].

Monolayer formation has in fact been thought to take place simultaneously by both random adsorption and nucleation growth [17]. We may term this model as the combined model (CM). The above work [17] presents some interesting chronoamperometric curves generated by this model. However, no LSV solution to this model was attempted.

We first present the current-potential expressions for the three models in a unified manner (Section 2). This is followed by the numerical solutions to these three models (Sec. 3). Since the differentiation between AM and NGOM has already been dealt with [15] we will only discuss the distinct features of CM in detail.

## 2. THE MODEL

Let us presume, for an oxidation process, that the monolayer M - A on a metal substrate M is formed by a one-electron oxidation of anion $A^-$ according to

$$M + A^- \rightleftarrows M - A + e^- \qquad \ldots (1)$$

$$(1 - X) \quad (X) \qquad \ldots (AM)$$

$$(1 - S) \quad (S) \qquad \ldots (NGOM)$$

This oxidation process can take place only on the free surface of the metal M [9 - 15]. We denote the fraction of the surface covered by adsorption as X and the fraction of the surface covered by NGOM as S. Hence the uncovered fraction of the surface in the AM is $(1 - x)$. We also presume for simplicity that the symmetry factor for the electrochemical reaction (1) is 0.5. Now we shall write down the current potential relations for the three models.

### 2.1 The adsorption model

The current at any time t is proportional to the surface coverage at that time and hence

$$i_a = q_{m,a} \frac{dX}{dt} \qquad \ldots (2)$$

where $i_a$ is the current due to adsorption, $q_{m,a}$ is the charge required for the monolayer coverage and dX/dt is the rate of change of surface coverage which is given by

$$\frac{dX}{dt} = k'_a C_{A^-} (1 - x) \exp\left[\frac{\eta}{b} + \frac{gX}{2}\right] - k_a x \exp - \left[\left(\frac{\eta}{b} + \frac{gX}{2}\right)\right] \qquad \ldots (3)$$

where $k'_a$ and $k_a$ are the adsorption and desorption rate constants of reaction (1), $C_A$ − is the concentration of the anion $A^-$, $\eta$ is the potential at any time t and is given by

$$\eta = E_i + \nu t \qquad \ldots (4)$$

since $E_i$ is presumed to be zero in the present work and $\nu$ is the sweep rate in volt sec$^{-1}$. In eq. (3) $b = RT/\beta F$, where $\beta$ is the symmetry factor presumed to be 0.5 and g is the lateral interaction parameter of the adsorbed species. A positive value of g is assumed for attractive interaction. It may be noticed that $k'_a$ and $k_a$ have different units in eq. (3). However, if we assume that $C_A^-$ is unity [10] and $k'_a C_A = k_a$, we obtain a much simpler expression for dX/dt.

$$\frac{dX}{dt} = k_a\left[(1-x)\exp\left(\frac{\nu t}{b}+\frac{gX}{2}\right) - x\exp-\left[\left(\frac{\nu t}{b}+\frac{gX}{2}\right)\right]\right] \qquad \ldots (5)$$

Equations (2) and (5) may be solved to obtain the current-potential expression for adsorption models.

### 2.2 The nucleation-growth overlap model

As in the adsorption model, the current at any time, t is given by

$$i_n = q_{m,n}\frac{dS}{dt} \qquad \ldots (6)$$

where $q_{m,n}$ is the maximum charge required for surface coverage. In the present model, however, the function dS/dt cannot be written in a straightforward manner as in AM (Sec. 2.1). We must model nucleation, growth and overlap independently to obtain the final expression for dS/dt.

#### 2.2.1 Rate of nucleation

The rate of nucleation or the number of nuclei (N) formed at any time t would be a function of surface coverage S at that time and the potential

$$\frac{dN}{dt} = f(s,\eta,t) \qquad \ldots (7)$$

In the earlier works on NGOM [7-8] the nucleation rate was presumed to be independent of surface coverage. The need to include the factor as a $(1-S)$ term in the nucleation rate expressions has been noted [13]. There were some interesting discussions on this point [18-20]. However, it is agreed that a more general nucleation rate expression must be considered [21] whereever the nucleation rate constant is very slow. However, if the nucleation rate is very fast (instantaneous nucleation) we may write

$$\frac{dN}{dt} = N_o\,\delta(t) \qquad (8)$$

In the present work, we will consider only this instantaneous nucleation case. In the above expression $N_o$ is the number of active centres.

#### *2.2.2 Growth of lone centers*

During monolayer formation by NGOM, it is assumed that the nuclei grow radially. Hence, the growth rate is related to the rate of change of radii of the active centres with time. The rate expression normally employed is [12, 14, 15]

$$\frac{dr}{dt} = \frac{M}{\varrho}\frac{1}{ZF}k'_g\left[\exp\left(\frac{\eta}{b}\right) - \exp\left(-\frac{\eta}{b}\right)\right] \qquad \ldots (9)$$

where M is the molecular weight, $\varrho$ is the density and $k'_g$ is the growth rate constant. However, it would be more convenient to employ the expression [18].

$$\frac{dr}{dt} = \alpha\, k_g\left[\exp\left(\frac{\eta}{b}\right) - \exp\left(-\frac{\eta}{b}\right)\right] \qquad \ldots (10)$$

In this expression $\alpha$ has the dimension of length and is given by $1/\sqrt{N_T}$ where $N_T$ is the total number of substrate atoms present per square centimeter of surface area. Following the above work [13] we assume that $N_T = 10^{15}/\text{cm}^2$ which gives an $\alpha$ value of $3.162 \times 10^{-8}$ cm and $q_{m,n}$ of 160 $\mu c/\text{cm}^2$. We also assume that each active nucleus contains only one atom [13]. Larger size nuclei would not change the qualitative behaviour of the simulated curves [13].

From the radial growth rate (eq. 10) we can obtain the area of each nucleus at any time as

$$\text{Area} = \pi\left[\int_y^t \left(\frac{dr}{dt}\right)_z dz\right]^2 \qquad (11)$$

The extended surface area $S_x$ of all such nuclei may be obtained by combining nucleation rate and growth rate as, [14]

$$S_x = \pi\int_o^t dy\left[\int_y^t \left(\frac{dr}{dt}\right)_z dz\right]^2 \left(\frac{dN}{dt}\right)_y \qquad \ldots (12)$$

For instantaneous nucleation, using equations 8, 10, 12, we obtain,

$$S_x = \pi N_o(\alpha k_g)^2\left[\int_o^t\left\{\exp\left(\frac{\nu t}{b}\right) - \exp\left(-\frac{\nu t}{b}\right)\right\} dz\right]^2 \qquad \ldots (13)$$

$$= 4\pi N_o\left(\frac{\alpha k_g}{V}\right)^2 \sinh^4 Vt \qquad \ldots (14)$$

$$= 4\,B\sinh^4 Vt \qquad \ldots (15)$$

where $V = \frac{\nu}{2b}$ and $B = N_o\left(\frac{\alpha k_g}{V}\right)^2$

#### 2.2.3. Real area of growth

When two growing centres contact each other, no further growth process can take place beyond the contact points of growing centres. However, mathematically this actual growth area (S) can be calculated from the total area of growth of centres $S_x$. This may be done by various methods [22, 23]. Both the approaches have recently been proved to be physically equivalent [14]. Using one of the expressions [22] we may write

$$S = 1 - \exp(-S_x) \qquad \ldots (16)$$

and hence

$$\frac{dS}{dt} = \exp(-S_x)\frac{dS_x}{dt} \qquad \ldots (17)$$

Using equation (17) in equation (16) where $S_x$ is given by equation (15) we may obtain the current potential relation from NGOM.

### 2.3. Combined model

In the combined model the total current would be equal to the current due to adsorption process ($i_a$) and nucleation process ($i_n$) [17]

$$i_c = i_a + i_n \qquad \ldots (18)$$

$$= q_{m,a}\frac{dX}{dt} + q_{m,l}\frac{dS}{dt} \qquad \ldots (19)$$

The dS/dt is agian given by the NGOM expression given earlier (Sec. 2.2.2.). The dX/dt expression would be slightly modified since the fraction S of the surface covered by nucleation also would not be available for growth and hence instead of equation (5) we write,

$$\frac{dx}{dt} = k_a\left[(1-S-X)\exp\left(\frac{\nu t}{b}+\frac{gX}{2}\right) - X\exp\left\{-\left(\frac{\nu t}{b}+\frac{gX}{2}\right)\right\}\right] \qquad \ldots (20)$$

The pseudocapacitance [10] may be calculated from $i_c$ using the expression

$$C\phi = i_c / v \qquad .. (21)$$

For each time t, $S_x$ was calculated using eq. (15). Eq. (16) then gives S. This allows eq. (20) to be solved by Runge Kutta 4th order differential method, numerically. Using this value and dS/dt value obtained from (17) we may obtain i using (19). $C\phi$ is then calculated using (21). In all these calculations $q_{m,a} = q_{m,n} = 160\,\mu c/cm^2$ was assumed. 1/b value at 25° C was 19.48 $V^{-1}$ since $\beta$ was assumed to be 0.5. Hence the variable parameters in the models were $k_a$ and g from the adsorption model, $k_g$ and $N_o$ in the NGO Model and the sweep rate $v$, the experimental parameter of the LSV technique.

The complete program (in BASIC) used in the numerical simulation work is given in Appendix I.

## 3. RESULTS AND DISCUSSION

As discussed earlier eq- (19) is the most general model for monolayer formation. By proper choice of $k_a$, $k_g$, g, $N_a$ and $v$, however, we can evaluate individual models and the influence of model parameters. In the following we shall discuss LSV characteristics of AM (Sec. 3.1), NGOM (Sec. 3.2) the influence of sweep rate on AM and GM (Sec. 3.3) and finally the CMF (Sec. 3.4)

### 3.1. Adsorption model

The LSV characteristics of AM may be obtained when $N_o$ and/or $k_g$ is taken to be zero. The LSV behaviour is now controlled by two model parameters $k_a$ and g.

The influence of $k_a$ on LSV behaviour is presented in Fig. 1 a.

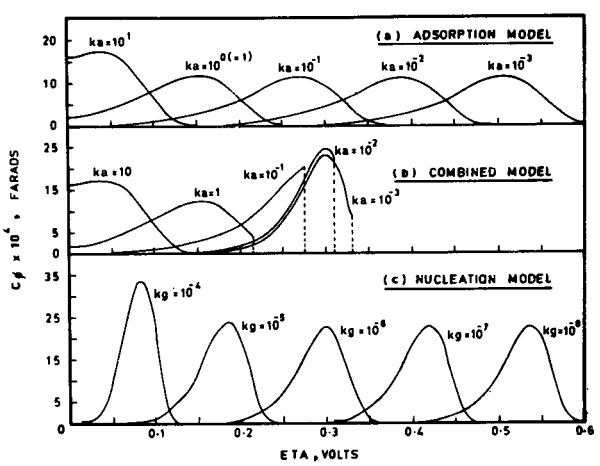


Fig. 1 : a) Influence of $k_a$ on LSV behaviour. AM.
No. = $10^{12}\,cm^{-2}$; $k_g = 0$; g = 0; $v = 1\,V sec^{-1}$

Fig. 1 : b) Influence of $k_a$ on LSV behaviour. CM.
No. = $10^{12}\,cm^{-2}$; $k_g = 10^{-6}\,sec^{-1}$; g = 0; $v = 1\,V sec^{-1}$

Fig. 1 : c) Influence of $k_a$ cn LSV behaviour. NGOM.
No. = $10^{12}\,cm^{-2}$; $k_a = 0$; g = 0; $v = 1\,V sec^{-1}$

When $k_a$ value is greater than $10^2 sec^{-1}$, the increasing portion of the voltammogram is not noticed. The current maximum occurs when $\eta = 0$ or the system behaves reversibly. When $k_a < 1$ the pseudo capacitance ($c\phi$) becomes independent of sweep rate and the peak potential shifts by approximately 118 mV per decade change of $k_a$ (Fig. 1a and Table 1)

Table I : Influence of $k_a$ on the LSV behaviour
Adsorption effect only. $N_o = 0$, $k_g = 0$, g = 0, $v = 1$

| $k_a$ $sec^{-1}$ | $i_p \times 10^4$ Amp | $C\phi \times 10^4$ Farad | $E_p$ Volt | (X + S) at $E_p$ |
|---|---|---|---|---|
| $10^2$ | | | No peak | |
| $10^{-1}$ | 17.30 | 17.30 | 0.04 | 0.416 |
| 1 | 12.08 | 12.08 | 0.155 | 0.629 |
| $10^{-1}$ | 11.52 | 11.52 | 0.27 | 0.624 |
| $10^{-2}$ | 11.46 | 11.46 | 0.39 | 0.638 |
| $10^{-3}$ | 11.45 | 11.45 | 0.505 | 0.615 |

When $10^2 > k_a > 1$ the system shows quasireversible behaviour. In the earlier works of simulations [10, 11] similar voltammetric behaviour is reported. However, these works have dimensionless parameters as the variable. The present work hence probably suggests the real limits of the $k_a$ values where reversible, irreversible and quasireversible behaviour is noticed.

The influence of g on the LSV bahaviour is presented in Fig. 2 fo r a $k_a$ value of 1.

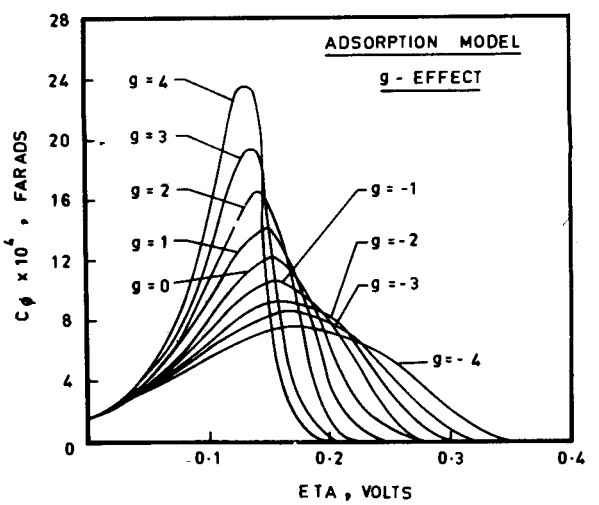


Fig. 2 : Influence of g on LSV behaviour. AM
$N_o = 10^{12} cm^{-2}$; $k_a = 1\ sec^{-1}$; $k_g = 0$; $v = 1\,V sec^{-1}$

The positive g values corresponding to attractive lateral interactions shift the peak potential to positive values and the peak current also increases (Table II, figure 2). The half peak width also decreases substantially with lateral attraction between adsorbates. Another characteristic feature is that the surface coverage at $E_p$ (X value) is greater than 0.66 for attractive interactions. In this respect as well, the present work agrees with the earlier simulation work [10].

### 3.2 Nucleation-growth-overlap model

The LSV characteristics of NGOM may be obtained from the general expression (eq. 19) when $k_a$ is taken to be zero. The voltammetric behaviour is then controlled by $k_g$ and $N_o$.

Table II: Influence of g on the voltammetric behaviour
Adsorption effect only. $N_o = 10^{12}$, $k_a = 1$, $k_g = 0$, $\nu = 1$

| g | $i_p \times 10^4$ Amp | $C_\phi$ Farad | $E_p$ Volt | X + S at $E_p$ |
|---|---|---|---|---|
| 4 | 23.35 | 23.35 | 0.13 | 0.730 |
| 3 | 19.44 | 19.44 | 0.135 | 0.686 |
| 2 | 16.36 | 16.36 | 0.14 | 0.649 |
| 1 | 13.96 | 13.96 | 0.145 | 0.618 |
| 0 | 12.08 | 12.08 | 0.155 | 0.629 |
| −1 | 10.58 | 10.58 | 0.16 | 0.601 |
| −2 | 9.36 | 9.36 | 0.165 | 0.577 |
| −3 | 8.36 | 8.36 | 0.17 | 0.556 |
| −4 | 7.53 | 7.53 | 0.175 | 0.561 |

The influence of growth rate constant $k_g$ on the LSV behaviour when $N_o = 10^{12}cm^{-2}$ is presented in Fig. 1.c. When $k_g \geq 10^{-2}sec^{-1}$ the rising portion of the voltammetric curve is not noticed. This shows that the system behaves reversibly under these conditions. (Table III)

Table III: Influence of $k_g$ on the LSV behaviour
Nucleation-growth effect only. $N_o = 10^{12}$, $k_a = 0$, $g = 0$, $\nu = 1$

| $k_g$ $sec^{-1}$ | $i \times 10^4$ Amp | $C_\phi \times 10^4$ Farad | $E_p$ Volt | X + S $E_p$ |
|---|---|---|---|---|
| $10^{-2}$ | No peak | | | |
| $10^{-3}$ | 80.68 | 80.6 | 0.03 | 0.639 |
| $10^{-4}$ | 33.73 | 33.73 | 0.085 | 0.620 |
| $10^{-5}$ | 24.20 | 24.20 | 0.185 | 0.630 |
| $10^{-6}$ | 23.03 | 23.03 | 0.3 | 0.619 |
| $10^{-7}$ | 22.90 | 22.90 | 0.42 | 0.648 |

However, this $k_g$ value is not unique as the $k_a$ value defined in the earlier section since here the reversibility may be obtained for a lower $k_g$ value as *well if $N_o$ is greater and vice versa. When $k_g < 10^{-2}sec^{-1}$ the peak shows* irreversible and quasireversible behaviour (Table III). The influence of $N_o$ on LSV when $k_g = 10^{-6}sec^{-1}$ may be noticed in Table IV

*Table IV: Influence of $N_o$ on LSV behaviour*
$k_a = 0$, $k_g = 10^{-6}$, $g = 0$ $\nu = 1$

| $N_o$ | $i \times 10^4$ Amp | $C_\phi \times 10^4$ Farad | $E_p$ Volt | X + S at $E_p$ |
|---|---|---|---|---|
| $10^{14}$ | 33.73 | 33.73 | 0.085 | 0.621 |
| $10^{13}$ | 24.20 | 24.20 | 0.185 | 0.630 |
| $10^{12}$ | 23.03 | 23.03 | 0.3 | 0.619 |
| $10^{11}$ | 22.91 | 22.91 | 0.42 | 0.648 |
| $10^{10}$ | 22.82 | 22.83 | 0.535 | 0.601 |

When $N_o \leq 10^{12}cm^{-2}$ the peak current becomes independent of $N_o$ and peak shift again reaches 119 mV/decade change.

### 3.3 Influence of sweep rate on AM and NGOM

At otherwise identical conditions the peak current decreases with the sweep rate for both the models (Table V and VI). At higher sweep rates both the models give pseudo capacitance values which are almost independent of sweep rate. However, at low sweep rates the $C\phi$ value continuously increases with sweep rate [15].

Table V: Influence of $\nu$ (sweep rate) on the voltammetric behaviour
$N_o = 10^{12}$, $k_a = 10^{-3}$, $k_g = 0$, $g = 0$

| $\nu$ Volt $sec^{-1}$ | $i \times 10^4$ Amp | $C_\phi \times 10^4$ Farad | $E_p$ Volt | X + S at $E_p$ |
|---|---|---|---|---|
| 1 | 11.44 | 11.44 | 0.505 | 0.615 |
| $10^{-1}$ | 1.46 | 11.46 | 0.39 | 0.638 |
| $10^{-2}$ | 0.115 | 11.51 | 0.27 | 0.624 |
| $10^{-3}$ | 0.0121 | 12.07 | 0.155 | 0.629 |

Table VI: Influence of $k_g$ on the voltammetric behaviour
$k_g = 10^{-8}$, $k_a = 0$, $g = 0$, $N_o = 10^{12}$

| $\nu$ Volt $sec^{-1}$ | $i \times 10^4$ Amp | $C_\phi \times 10^4$ Farad | $E_p$ Volt | X + S at $E_p$ |
|---|---|---|---|---|
| 1 | 22.84 | 22.84 | 0.535 | 0.601 |
| $10^{-1}$ | 2.29 | 22.90 | 0.42 | 0.648 |
| $10^{-2}$ | 0.23 | 23.03 | 0.30 | 0.619 |
| $10^{-3}$ | 0.024 | 24.20 | 0.185 | 0.630 |

In all these aspects, the simulated LSV cruves of AM and NGOM closely correspond to the results reported earlier [9 - 15]. This establishes the fact that the overall expression eq. (19) is essentially correct and should represent the combined model.

### 3.4 The combined model

When $k_a$, $k_g$ and $N_o$ all have non-zero values, the LSV behaviour represented by equation (19) corresponds to the combined model. Since $i_c$ in this model is the addition of adsorption and nucleation components, the predominance of these components controls the overall current $i_c$. This is clearly noticed in Fig. 1. Fig. 1 - 6 presents the current-potential curves for the combined model for a constant value of $k_g$ ($10^{-6}sec^{-1}$) and varying values of $k_a$. For $k_a \geq 1$ *the overall curves are* quire similar to the curves in Fig. 1a with same $k_a$ values. For $k_a = 10^{-1}$ where $E_p$ for NGOM (0.3 V, see Fig. 1.a and 1.c) the current is found to increase continuously and drop suddenly to zero within the next 5 mV interval. Similar sudden drop in current is also notices for $k_a = 10^{-2}sec^{-1}$. For $k_a < 10^{-2}sec^{-1}$ the current component due to $k_a$ would decrease substantially and the peak current of the combined model corresponds to the NGO model (compare Fig. 1b and 1c). It must also be noted that the X + S value or the total surface coverage value is substantially greater than 0.66 (Table VII).

Table VII: Influence of $k_a$ effect on the voltammetric behaviour combined model
$N_o = 10^{12}$, $k_g = 10^{-6}$, $g = 0$, $\nu = 1$

| $k_a$ $sec^{-1}$ | $i_p \times 10^4$ Amp | $C_\phi \times 10^4$ Farad | $E_p$ Volt | X + S at $E_p$ |
|---|---|---|---|---|
| $10^2$ | 17.30 | 17.30 | 0.04 | 0.416 |
| 1 | 12.20 | 12.20 | 0.155 | 0.631 |
| $10^{-1}$ | No peak | | | |
| $10^{-2}$ | 24.47 | 24.47 | 0.3 | 0.740 |
| $10^{-3}$ | 23.23 | 23.23 | 0.3 | 0.633 |
| $5 \times 10^{-2}$ | | No peak | | |
| $5 \times 10^{-3}$ | 23.90 | 23.90 | 0.3 | 0.683 |

**APPENDIX-I**

```
E>
100 REM ADSORPTION - NUCLEATION MODEL
110 DIM R(500),X(1000),T(1000),SHVT(500),CHVT(500),S(500)
120 READ T(1),X(1),H,NMAX
130 READ V1,AL,KG,KA,NO,QM,QA,G
140 V=.25*38.93*V1
150 B=3.1415*((AL*KG*NO)^2/V^2)
160 LPRINT "KA=";KA,"KG=";KG
170 LPRINT "V1=";V1,"NO=";NO,"G=";G,"QM=";QM
175 LPRINT
180 LPRINT TAB(2);"S+X";TAB(16);"ETA";TAB(33);"IC";TAB(50);"CAP"
200 FOR N=1 TO NMAX
210 T=T(N)
220 X=X(N)
230 GOSUB 470
240 S1=H*F
250 T=T(N)+H/2
260 X=X(N)+S1/2
270 GOSUB 470
280 S2=H*F
290 T=T(N)+H/2
300 X=X(N)+S2/2
310 GOSUB 470
320 S3=H*F
330 T=T(N)+H
340 X=X(N)+S3
350 GOSUB 470
360 S4=H*F
370 T(N+1)=T(N)+H
380 X(N+1)=X(N)+(S1+2*S2+2*S3+S4)/6
390 GOSUB 530
400 ICA1=QA*KA*((R(N)-X(N))*EXP(2*V*T(N)+G*X(N)/2))
405 ICA2=-QA*KA*X(N)*EXP(-2*V*T(N)-G*X(N)/2)
410 ICN=16*B*QM*V*R(N)*SHVT(N)^3*CHVT(N)
420 IC=ICA1+ICA2+ICN
430 ETA=V1*T(N)
435 C=IC/V1
436 XS=1-R(N)+X(N)
450 LPRINT X+S;TAB(15);ETA;TAB(30);IC;TAB(45);C
460 NEXT N
470 SHVT=(EXP(V*T)-EXP(-V*T))/2
480 SX=4*B*(SHVT)^4
490 S=1-EXP(-SX)
495 IF S+X)=1 OR S)=1 THEN STOP
500 R=1-S
510 F=KA*((R-X)*EXP(2*V*T+G*X/2)-X*EXP(-2*V*T-G*X/2))
520 RETURN
530 SHVT(N)=(EXP(V*T(N))-EXP(-V*T(N)))/2
540 CHVT(N)=(EXP(V*T(N))+EXP(-V*T(N)))/2
550 SX=4*B*(SHVT(N))^4
560 S(N)=1-EXP(-SX)
570 R(N)=1-S(N)
580 RETURN
590 DATA 0,0,.005,300
600 DATA 1,3.16E-08,1E-03,1E-01,1E12,1.6E-04,1.6E-04,0
610 STOP
620 END
```

When $k_a$ was kept constant and $k_g$ was gradually reduced, the peak current of the combined model was found to change from predominantly NGO control to adsorption control. The behaviour was very similar to the one reported above (Table VIII).

Table VIII: Influence of $k_g$ on the voltammetric behaviour combined model

$N_o = 10^{12}$ $k_a = 10^{-1}$ $g = 0$ $v = 1$

| $k_a$ $Sec^{-1}$ | $i_p \times 10^{14}$ Amp. | $C\phi \times 10^4$ Farad | $E_p$ Volt | X + S |
|---|---|---|---|---|
| $10^{-3}$ | 80.78 | 80.78 | 0.03 | 0.642 |
| $10^{-4}$ | 34.03 | 34.03 | 0.085 | 0.637 |
| $10^{-5}$ | 25.63 | 25.63 | 0.185 | 0.754 |
| $5 \times 10^{-6}$ | 25.55 | 25.55 | 0.215 | 0.784 |
| $10^{-7}$ | 11.64 | 11.64 | 0.27 | 0.626 |
| $10^{-8}$ | 11.52 | 11.52 | 0.27 | 0.589 |

All the parameters were closely varied to see if under any specific condition two peaks could be obtained. However, no such condition was found to exit.

## 4. CONCLUSIONS

A general LSV expression for AM, NGOM and CM was obtained in the present work. By proper selection of parameters this expression could be used to generate LSV curves for AM, NGOM and CM. The LSV behaviour of CM which is being reported for the first time suggests at least two criteria to distinguish this model from the other two models. When both adsorption and nucleation processes operate, the current shows a monotonous increase and suddenly drops to zero. This behaviour is not at all noticed in NGO or Adsorption model. Secondly the surface coverage at $E_p$ would be greater than 0.66 whenever CM operates. This condition would not arise in NGO Model. However, in the AM when $g > 2$ the X + S could reach values greater than 0.66. In this case, the current peaks would be sharp and quite symmetric (Fig. 2) which would enable one to distinguish between AM and CM. As long as no induced heterogeneity effects are present, in the combined model also only one LSV peak is noticed. The effect of surface heterogeneity on LSV characteristics in combined model is being investigated at present and would be reported shortly.

## REFERENCES


1. D Kolb, *Advances in Electrochem and Electrochem Eng.*, Vol. II (H Gerischer and C Tobias Ed.) Wiley, New York (1978) p 125
2. K Juttner and W J Lorenz, *Z Phys Chem*, NF **122** (1980) 163
3. M Fleischmann and H R Thirsk, *Advances in Electrochem and Electrochem Eng*, Vol 3 (P Delahay Ed) Wiley, New York (1963) 123
4. J A Harrison and H R Thirsk, *Electroanal Chem*, Vol 5 (A J Bard Ed) Marcel Dekker, New York (1972)
5. P Will and C A Knorr, *Z Elektrochem*, **64** (1960) 254
6. S Gilman, *Electroanal Chem*, Vol 2 (A J Bard Ed) Marcel Dekker, New York (1967) 111
7. G Belanger and A K Vijh, *Oxides and Oxide Films*, Vol 5 (A K Vijh, Ed) Marcel Dekker, New York (1977) 1
8. R Woods, *Electroanal Chem*, Vol 9, (A F Bard, Ed) Marcel Dekker, New York (1976) 1
9. S Srinivasan and E Gileadi, *Electrochim Acta*, **11** (1966) 321
10. H Angerstein Kozlowska, J Klinger and B E Conway, *J Electroanal Chem*, **75** (1977) 45
11. H Angerstein Kozlowska and B E Conway, *J Electroanal Chem*, **95** (1979) 1
12. S K Rangarajan, *Faraday Symp of Chem Soc*, **12** (1978) 103
13. H Angerstein-Kozlowska, B E Conway and P Klinger, *J Electroanal Chem*, **87** (1978) 301
14. E Bosco and S K Rangarajan, *J Chem Soc Faraday Trans*, **1** (1981) 483
15. E Bosco and S K Rangarajan, *J Electroanal Chem*, **129** (1981) 25
16. *Faraday Symp Chem Soc*, **12** (1978)
17. E Bosco and S K Rangarajan, *J Chem Soc Faraday Trans*, **1** 77
18. D R Armstrong, A Bewick and M Fleischmann, *J Electroanal Chem*, **99** (1979) 375
19. L de Silva Pereira and L M Peter, *J Electroanal Chem*, **99** (1979) 377
20. H Angerstein-Kozlowska, B E Conway and J Klinger, *J Electroanal Chem*, **99** (1979) 381
21. M Y Abyaneh and M Fleischman, *J Electroanal Chem*, **119** (1981) 187
22. M Avrami, *J Chem Phys*, **7** (1939) 1103
23. U R Evans, *Trans Faraday Soc*, **41** (1945) 365